Indirect (n,γ) cross sections of thorium cycle nuclei using the surrogate method

J. N. Wilson, F. Gunsing, L. A. Bernstein, A. Bürger, A. Görgen, M. Guttormsen, A-C. Larsen, P. Mansouri, T. Renstrøm, S. J. Rose, A. Semchenkov, S. Siem, N. U. H. Syed, H. K. Toft, M. Wiedeking, and T. Wiborg-Hagen

Phys. Rev. C **85**, 034607 — Published 15 March 2012

DOI: 10.1103/PhysRevC.85.034607

Indirect (n,γ) cross sections of thorium cycle nuclei using the surrogate method

J.N. Wilson [a], F. Gunsing [b], L.A. Bernstein [d], A. Bürger [c], A. Görgen [b,c], M. Guttormsen [c], A-C. Larsen [c], P. Mansouri [c], T. Renstrøm [c], S.J. Rose [c], A. Semchenkov [c], S. Siem [c], , N.U.H. Syed [c], H.K. Toft [c], M. Wiedeking [d,e], T. Wiborg-Hagen [c]

[a] *Institut de Physique Nucléaire d'Orsay, Bât. 100, 15 rue G. Clémenceau, 91406 Orsay cedex, France*
[b] *CEA Saclay , DSM/Irfu, F-91191 Gif-sur-Yvette Cedex, France*
[c] *University of Oslo, Department of Physics, P.O. Box 1048, Blindern 0316 Oslo, Norway*
[d] *Lawrence Livermore National Laboratory, 7000 East Avenue, Livermore, CA 94550-9234, USA*
[e] *iThemba LABS, P.O. Box 722, 7129 Somerset West, South Africa*

Indirect neutron capture (n,γ) cross sections have been extracted for the key thorium cycle nuclei ^{232}Th, ^{231}Pa and ^{230}Th using the surrogate reaction method. Final nucleus gamma decay probabilities were measured between the neutron binding energy and around 1MeV above it using the ^{232}Th(d,p)^{233}Th, ^{232}Th(^{3}He,t)^{232}Pa and ^{232}Th(^{3}He,α)^{231}Th reactions in experiments with the Cactus gamma-detector array and Silicon Ring charged particle detectors at the Oslo Cyclotron Laboratory. Since the neutron capture cross section for ^{232}Th is already well known from direct measurements a comparison with these results provides a stringent test of the applicability of the surrogate method in the actinide region for indirect (n,γ) cross section measurements. In addition, a new technique for correcting measured gamma ray decay probabilities below the neutron emission energy threshold is proposed and used. We find good agreement between indirect and direct (n,γ) cross section measurements in the range 500 keV – 1 MeV, but large discrepancies outside this range. Explanations for the observed differences are proposed.

PACS number(s): 24.87.+y, 24.10.-i, 25.45.-z, 25.55.-e

I. INTRODUCTION

Nuclear cross section data in the actinide region are vital for precise simulations of nuclear reactors. The modeling of core reaction rates, nuclear fuel depletion and the extraction of reactor performance parameters, rely on accurate cross section data over a large range in energy, from thermal neutrons (10^{-4} eV) to fast neutrons (10^{7} eV). While direct neutron induced cross section measurements have been carried out on major fissile and fertile isotopes in the actinide region, for many short lived isotopes the available cross section data are either partial, uncertain or in some cases missing entirely. In such cases the various evaluated date bases (ENDF, JEFF, JENDL, etc.) rely heavily on theoretical calculations which can produce values which are in disagreement by sometimes an order of magnitude. Many actinide nuclei synthesized in nuclear reactor cores have relatively short half lives (< 100 years) and hence very high activities (> 1 G Bq/μg). Thus many cross sections remain unmeasured or have large uncertainties due to the technical problems of preparing and handling the highly radioactive targets required for direct cross section measurements.

The surrogate method [1] is an indirect measurement technique proposed in the 1970's to overcome these problems, in which a transfer reaction involving light charged particles in the entrance and exit channels is substituted for a direct neutron-induced reaction to produce the same final nuclear system. If the energies of the ingoing and outgoing charged particles are known or measured, then the excitation energy E_x of the final nucleus can be deduced and can be related to the equivalent incident neutron energy E_n in the following way:

$$E_n = \frac{A+1}{A}(E_x - S_n) \quad (1)$$

for a target nucleus of target mass A and neutron binding energy S_n. The exit channel via which the final nucleus decays can then be detected with a suitable detection system.

Recently, this method has been successfully used for indirect measurements of neutron-induced fission, (n,f), cross sections for several actinide nuclei [2,3,4]. However, for neutron-induced capture, (n,γ), cross sections only one measurement in the actinides, ^{233}Pa(n,γ), has been attempted due to the particular technical difficulties of the surrogate technique [5]. Another (n,γ) measurement has been performed using the surrogate ratio method (SRM) to extract indirectly the ^{235}U(n,γ) cross section [6]. The surrogate ratio method [7,8,9,10] is a different technique which relies on a comparison of two neighboring final nuclei created under the same experimental conditions, where one of the surrogate cross sections is known from direct measurements.

Recently, the surrogate method for (n,γ) cross sections on isotopes of Gadolinium (^{154}Gd, ^{156},Gd and ^{158}Gd) has been tested [11], where significant differences between direct and indirect cross sections at low energies (< 1 MeV) were observed. Hauser-Feshbach calculations indicated that these large differences occur because of the mismatch in the angular momentum, J, and parity, π, distributions of the final nuclei produced in the indirect and direct reactions. However, it is not clear whether these discrepancies also exist in actinide nuclei where masses and level densities are higher than in the rare earth region and the problem should presumably be less severe.

In this paper we report on results from surrogate-method (n,γ) cross section measurements for key thorium cycle nuclei at the Oslo Cyclotron Laboratory using the Cactus and Silicon Ring detectors.

II. THE SURROGATE METHOD

The neutron capture cross section $\sigma_{(n,\gamma)}$, can be broken into two parts (eqn. 2), where a sum over all spins and parities, J,π is made for the compound nucleus formation cross section multiplied by a decay probability , P_γ for gamma cascades to the ground state.

$$\sigma_{(n,\gamma)}(E_n) = \sum_{J,\pi} \sigma_{CN}(E_n, J, \pi) P_\gamma(E_n, J, \pi) \tag{2}$$

In the Weisskopf-Ewing approximation where the decay probability is assumed to not vary with spin and parity this simplifies to the following expression:

$$\sigma_{(n,\gamma)}(E_n) = \sigma_{CN}(E_n) P_\gamma(E_n) \tag{3}$$

In theoretical cross sections calculations the quantity that is difficult to determine is the decay probability, P_γ, since it is heavily dependent on nuclear level densities and photon strength functions, which can vary rapidly with N and Z due to differences in nuclear structure such as deformation, etc. and are thus difficult to predict. Different level density models, although calibrated to the measured level spacing around the neutron binding energy, easily disagree by a factor of two [12] at higher or lower energies. The compound nucleus formation cross section, however, can be calculated from the optical model potential (OMP) which has been validated over a large range of nuclei in the valley of stability and typically differences between theory and experiment are around 10-20%. In the surrogate method, the decay probability is measured and then combined with a calculated or theoretical compound nuclear formation cross section to deduce the direct neutron-induced capture cross section. This means that surrogate method at best is only capable of extracting cross section information to within perhaps 15-20% accuracy due to the reliance on OMP compound nucleus formation section calculations. The Weisskopf-Ewing approximation that the decay probability is independent of spin and parity is precisely what we intend to test by a comparison by comparing surrogate method results to cross sections which are directly known.

The main problem with the surrogate method is that it assumes that any mismatches in the spin and parity distributions of the final nucleus when compared to the equivalent neutron-induced reaction will have no effect on the

decay probability. It is reasonable to suppose that the heavier the beam particle used in the surrogate reaction, the higher the maximum angular momentum brought into the final system and the greater likelihood of disagreement between surrogate and neutron-induced measurements. While the surrogate method appears to reproduce direct cross section measurements reasonably well for several (n,f) cross sections; three is still a question mark over its applicability for (n,γ) cross sections. In the actinide region (n,γ) cross sections are particularly difficult to measure because of the presence of gamma rays from fission and inelastic scattering which are impossible to distinguish from capture gamma rays. In this work indirect (n,γ) cross section measurements using the surrogate method are presented for ^{232}Th, ^{231}Pa and ^{230}Th using (d,p), (^{3}He,t) and (^{3}He,^{4}He) transfer reactions respectively.

III. EXPERIMENTS

The experiments were carried out at the Oslo Cyclotron Laboratory, where beams of deuterium and ^{3}He at bombarding energies of 12 MeV and 24 MeV respectively were incident on a 968 μg/cm^2 target of ^{232}Th. Gamma rays from the target position were detected with the Cactus spectrometer, a 4π array of 28 high efficiency lead-collimated NaI detectors arranged in a spherical geometry (see fig.1). The total detection efficiency of Cactus is approximately 15% with each cylindrical NaI detector having a diameter of 12.35 cm and length of 12.35 cm, the front face being situated at 22 cm from the central target position. Light charged particles emitted at backward angles from the beam direction were detected by the Silicon Ring detector [13], a ring of 8 wedge-shaped detector modules, each with 8 arced ΔE strips of 130 μm thickness placed in front of a single E detector of 1550 μm thickness. The eight annular rings of the silicon detectors were at angles of 124 degrees for the outermost ring and 138 degrees for the innermost, giving an angular resolution for charged-particle detection of slightly less than 2 degrees. The total solid angle covered by the silicon ring was approximately 12% of 4π steradians. An aluminum absorber of thickness 10.5 μm was placed in front of the silicon detectors block δ electrons originating from the target.

During the experiments all coincidence events involving at least one ΔE strip and at least one E detector were written to disk along with any coincident gamma ray data, if present. During the two weeks of beam time (approx. 1 week for d at 0.7 nA and 1 week for ^{3}He at 0.4 nA) a total of 351 million and 135 million ΔE-E coincidence events for d, and ^{3}He beams respectively, were recorded to disk. Particle identification of the outgoing charged particles (p,d,t, ^{3}He and α) was performed by setting two dimensional gates in the ΔE-E plane for each energy-calibrated annular ring of 8 detectors (see fig. 2.). After particle identification, the total number of particle-γ coincidence events collected were 23M, 0.79M and 0.57M for the channels of interest: (d,p)^{233}Th*, (^{3}He, α)^{231}Th* and (^{3}He,t)^{232}Pa* respectively.

A. Silicon detector energy calibration and data analysis

A ^{12}C target was also used with the d and ^{3}He beams to provide data points for energy calibrations in the laboratory frame of the 64 ΔE and 8 E detectors of the silicon ring. However it proved difficult to obtain a universal calibration for all channels simultaneously, probably due to small differences in charge collection (ballistic deficit) for the different detected particle types. For the (d,p) channel the best calibration coefficients were obtained by using the elastic scattering peaks on ^{232}Th(d,d') and^{16}O(d,d'), a target contaminant. For the (^{3}He,α) and (^{3}He,t) channels the silicon detector calibration coefficients were obtained from elastic scattering peak of ^{232}Th(^{3}He,^{3}He') and the position of the ^{232}Th(^{3}He,α) ^{231}Th* ground state. The energy of the final nucleus was then reconstructed for each event from the sum energy (ΔE+E) detected in the lab-frame, corrected for the energy losses in the target, aluminum absorber and the kinematics of the reaction. The energy resolution for detection of light charged particles assuming a 2mm beam spot size was 80 keV.

To facilitate the analysis 2-dimensional spectra were created with detected gamma ray energy on the x-axis correlated with final nuclear excitation energy on the y-axis. Background counts from events in which two or more different nuclear reactions occurred in the same cyclotron beam burst were subtracted from these matrices by gating on neighboring bursts in the spectrum of time differences measured between particle and gamma ray detection.

B. The Weighting function technique

The final nucleus decay probabilities were measured using the weighting function technique outlined in [14,15]. This technique has the advantage over methods using high-resolution spectroscopy to identify transition(s) near the ground state, because it does not introduce any bias by selecting final states of a certain spin.

Let us imagine a detector with a detection efficiency ε, that is proportional to incident gamma ray energy E_γ (see eqn. 4). Then for low multiplicity cascades of m gamma rays, where the isolated hit probability for the detector is assumed to be 1.0, the efficiency with which cascades are detected, ε_c would be the sum of the efficiencies of the individual energies $\varepsilon_{j=1..m}$ (eqn. 5) and thus independent of the cascade path for cascades which start with the same energy.

$$\varepsilon = kE_\gamma \tag{4}$$

$$\varepsilon_c \approx \sum_{j=1..m} \varepsilon_j \tag{5}$$

In practice no detector will have such a property, but the response, R, of a detector can be weighted with a function $W(E_d)$ which forces such a relationship for detected energies E_d:

$$\sum_{E_d} W(E_d) R(E_d, E_\gamma) = kE_\gamma \tag{6}$$

In this work, the response matrix for the Cactus array was found by performing detailed MCNP5 simulations of the Cactus detectors, the Pb collimators, the target and frame, the vacuum chamber and the detector casings for many different energies and then interpolating between them in a similar manner to that outlined in [14] (see fig. 3.) The response was broadened with a broadening function (eqn. 7) to provide the correct NaI detector resolution, which is not accounted for in the MCNP simulations since the scintillator light collection and photo-multiplier tube are not modeled.

$$w = aE + bE^2 \tag{7}$$

The coefficients a and b were determined from fits to the peak widths of experimental mono-energetic gamma spectra from excited states of ^{13}C and ^{17}O produced in the ^{12}C(d,p) and ^{16}O(d,p) reactions by gating on the appropriate proton energies.

To obtain a complete set of weighting functions the ideal solution would be to invert the detector response matrix. Unfortunately this matrix is singular due to the energy detection thresholds of the NaI detectors. In this work the downhill simplex method was used as a minimization procedure to find 6^{th} order polynomials which serve as the complete set of weighting functions between 100 keV and 10 MeV, since a unique weighting function is needed for each total cascade energy. It has been shown in [14] that the combined effect of imperfect weighting functions due to the presence of gamma detection thresholds and the fact that the detectors do not have isolated hit probability of 100% can lead to systematic uncertainties in the measurement technique of the order of 2% for relative (when comparing one cross section with another) and 5% in the absolute values.

C. Discrimination against neutrons

The NaI detectors of the Cactus array are not transparent to neutrons and there is the possibility that in some events where the final nucleus excitation energy is above S_n neutrons will be emitted and interact in the NaI detector by either an (n,n') or (n,γ) reaction. The (n,n') reaction is the most probable [16] but the energy deposited will be very low and these type of events have been energetically excluded by imposition of an appropriate energy threshold (see the following section). Neutron capture in the NaI presents a greater problem because it is followed by emission of a ~7 MeV cascade of gamma rays which will be wrongly weighted in the analysis. However, discrimination against these types of events can be made by neutron time of flight. The time resolution of Cactus detectors was determined from the cyclotron frequency of 47 ns between neighboring beam bursts. The size of the time window placed on the prompt gamma peak detected in Cactus was 22 ns, and since the average neutron interaction point in the NaI detector is 25cm from the target, then slow neutrons with energies less than 700 keV were excluded. For faster neutrons with energies greater than 700 keV, the neutron capture cross section in the NaI detector is at least an order of magnitude lower than the (n,n') cross section. Therefore, neutron capture in the NaI represents a tiny fraction of the events and thus will not contribute significantly to the error in the decay probability measurement.

D. Correction for (n,n') events

In the decay probability measurement of Boyer *et al.*[5], a correction was made to the measured decay probabilities of the ^{234}Pa final nucleus because of the difficulty of discriminating gamma decay to the ground state and emission of a neutron followed by gamma decay. The latter events are the equivalent of (n,n') events in the neutron induced reaction. The correction was performed to compensate for these gammas and was based entirely on model-dependent cross section calculations.

To avoid the decay probability measurement becoming model-dependent we present here a new correction technique based on extrapolation of the measured gamma ray spectrum to the lowest energies below the energy threshold where detection of gammas accompanied by neutron emission becomes energetically feasible. If a neutron is emitted, then the amount of available energy left for gamma decay is small. However, since the neutron is not detected there is no way of separating these events from those where decay proceeds by gamma emission alone. If a moving low energy threshold on the gamma ray spectrum is placed at E_x-S_n then exclusion of events where neutrons are emitted is assured. However, the higher the final nuclear excitation energy, the higher the threshold must be set and the more low energy gamma rays from capture will be excluded.

The proposed extrapolation technique relies on the assumption that the shape of the gamma ray spectrum below the energy threshold E_x-S_n is known. We assume that gamma rays below E_x-S_n are not primary gamma rays, but instead are secondary and tertiary gamma rays from transitions in the potential well nearer the ground state. This assumption is made because the spectral shape below the threshold (up to 1.2 MeV) is not observed to change as a function of E_x (see fig. 4). The extrapolation assumes an identical spectral shape as those in fig. 4 for $E_x > S_n$ for the low energy part of the gamma spectrum between E_γ=0 and $E_\gamma = (E_x\text{-}S_n)+\Delta$, where Δ is a small energy range just above threshold (50 – 100 keV) used to perform the normalization needed to perform the extrapolation. All counts in the combined spectrum (experimental spectrum above threshold and extrapolated spectrum below threshold) can then be weighted to extract the corrected decay probability (i.e. the probability of a gamma cascade to the ground state for each final nucleus produced). Fig. 5. shows the details of the extrapolation and weighting procedure at the highest threshold energy.

E. Contaminants and Deuterium breakup

One of the difficulties in analysis of surrogate method data is the presence of target contaminants, frequently ^{16}O and ^{12}C. Reactions involving these nuclei have high cross sections but are strongly forward focused, so detected particles from contaminant reactions can be minimized by placing charged particle detectors at backward angles, as was done in this work. In surrogate (n,γ) measurements the corresponding gamma-rays from the 1st, 2nd; etc. excited states of these nuclei can be indentified and the contribution from the contaminant reaction can be subtracted.

The peaks are broad and at the wrong energies because the kinematic correction is performed assuming a reaction involving a heavy actinide nucleus and not light contaminants. For reactions which leave the light contaminant

nucleus in its ground state e.g. $^{16}O(d,p)^{17}O$ seen at E_x = 4.5 MeV in fig. 6, there are no gammas emitted and hence correction and subtraction of these excess counts from the singles spectrum is difficult. In this experiment the peak occurred at 4.5 MeV, which is below the neutron binding energy of ^{232}Th and therefore did not interfere with the decay probability measurement. For $^{12}C(d,p)^{13}C$ the ground state occurs at an excitation energy in ^{233}Th of 6.5 MeV and is thus outside the energy range over which the measurement was performed.

It has also been suggested that some protons detected at backward angles may come from reactions involving the breakup of the deuterium in the Coulomb field of the target nucleus, and that these protons have the potential to distort the measurement in a similar manner to the presence of protons emitted in reactions on target contaminants. Fig. 6. shows that this is unlikely since we are able to count the number of cascades from the very lowest final nuclear excitation energies via detecting the protons, and again independently by weighting the coincident gamma rays via the weighting function technique. Below the binding energy the number of cascades counted varies substantially with energy but is almost identical for proton "singles" and coincident weighted gammas. If there were any excess of protons from breakup reactions with no coincident gammas then it would be observed as a difference in number of cascades between gammas and protons. We therefore conclude that protons from deuteron breakup reactions are not detected at backward angles and do not affect the results.

V. RESULTS

Fig. 7 shows the ejectile spectra for proton, tritum and alphas in coincidence with at least one gamma ray for the ^{233}Th, ^{232}Pa and ^{231}Th final nuclei respectively. Fig. 8. shows that the decay probabilities obtained from applying the weighting function technique to obtain the fraction of total events which decay via gamma emission to the ground state at a given equivalent neutron energy. The error bars on the decay probabilities are derived from the statistical fluctuations in the detected gamma spectrum where the effect of the very different weightings at different energies is correctly treated. The errors in the x direction are derived from the measured energy resolutions for detecting the different particle types in the silicon ring. If the set of weighting functions for the cactus detector are correct, then the measured decay probabilities below the neutron separation energy should all be consistent with unity. This is clearly the case for the $^{233}Th^*$ and $^{232}Pa^*$ data. For the $^{231}Th^*$ data, the first 7 data points are slightly higher with averaged value of value of 1.033 +/- 0.015. This is 2.2 standard deviations above unity but does not present a problem since it is consistent with unity to within the statistical and systematic uncertainties of the measurement technique (2% relative and 5% absolute).

The TALYS code[17] was used to obtain the compound nucleus formation cross sections for the equivalent neutron-induced reactions for the purpose of combing them with the measured decay probabilities to obtain the neutron-induced cross sections for $^{232}Th(n,\gamma)$ $^{231}Pa(n,\gamma)$ and $^{230}Th(n,\gamma)$. Using the optical model only, one can calculate the total cross section and the direct scattering cross section, while the difference corresponds to the reaction cross section which in this energy range is associated with the compound nucleus formation cross section. The direct scattering cross section is not directly observable since it is experimentally indistinguishable from the compound scattering cross section, part of the reaction cross section. Therefore only the total cross section can be used to be described by optical model calculations. The same optical model parameters can then be used to calculate the compound nucleus formation cross section, which is not present in evaluated data.

We have adjusted the optical model parameters in TALYS to reproduce the total cross sections as present in evaluated nuclear data libraries. For this purpose the TALYS calculations were included in a least-squares minimization procedure. For each iteration an input file with OMP parameters was generated and used for a TALYS calculation. The output file with the calculated total cross section was then compared to the evaluated total cross section on a logarithmically spaced energy grid covering the same unresolved resonance region as in the library. The optical model parameters which reproduced best the total neutron-induced cross section were then used to calculate the compound nucleus reaction cross section.

Although the measured decay probabilities presented here are independent quantities, their transformation to a capture cross section depends of course directly on the quality of the compound nucleus formation cross section which is used and therefore on the quality of the total cross section in the evaluated libraries.

Fig. 9. shows the results for the ^{232}Th(n,γ) surrogate method compared to the ENDFB7 database which is based on recent accurate measurements from both n_TOF [18] and GELINA [19, 20]. In the range 500 keV – 1 MeV there is very good agreement with variations typically of the order of 15%. Above 1 MeV the fission cross section begins to increase and since we are unable to distinguish events in which fission occurs, fission gamma rays will begin to contaminate our spectra. Thus it is not surprising that above 1 MeV the surrogate data increasingly overestimates the ENDFB7 database values. If fission detectors had been present to detect the gamma spectra correlated with fission events, then it would have been possible to correct for the presence of fission gamma rays. In future experiments we intend to include fission detectors in the experimental setup.

The major discrepancy between our measurements and ENDFB7 occur in the range 0 – 500 keV, where there is a large and increasing disagreement towards low energy as high as 400%. These results are similar to those obtained by Scielzo *et al.* in the Gadolinium nuclei [11], where again the largest discrepancies are seen to occur across the entire energy range, but most noticeably at the lowest energies. In their work Hauser-Feshbach calculations were performed to obtain the decay probabilities as a function of the spin and parity of the final nucleus. It was shown that the likely explanation of the observed discrepancies was due to the strong spin-dependence of the decay probability at low energies, and hence any angular momentum mismatch between the direct and indirect reactions would produce a large difference in the indirect and direct measurements because the highest *l*-waves favor gamma decay leading to an overestimate of the cross section. Hatarik *et al*. [10] have proposed a method where this overestimation of the decay probability is corrected via the subtraction of components from higher spin states and appears to be a promising line of further inquiry.

While the explanation of overestimation of decay probabilities appears reasonable and convincing we also propose an additional reason why discrepancies may exist at the lowest energies which may be due to the finite energy resolution of the charged particle detectors. We assume that the decay probability function that we are attempting to measure is well-approximated by a step function. Below the neutron binding energy, the decay probability is 1.0 and all decays proceed by gamma emission to the ground state. Above the binding energy other decay channels become immediately open (e.g. neutron emission) and thus the gamma decay probability rapidly drops to a value lower than unity at the neutron binding energy. If detectors have a finite energy resolution then the step function will be smoothed out and a measured value of the decay probability P_m at a given equivalent neutron energy, E_n will be an admixture of the actual value P_a and 1.0, the value below the neutron binding energy for all negative values of E_n:

$$P_m(E_n) = g \times P_a(E_n) + (1-g) \times 1.0 \tag{8}$$

where g is the integral of the Gaussian function which represents the detector resolution:

$$g = \frac{1}{\sqrt{2\pi}} \int_{-\infty}^{E_n} e^{-E_n/2w} dE_n \tag{9}$$

It is thus possible to correct backwards for this smoothing effect of the detectors from the measured detector resolution, w. This correction has been performed for the ^{232}Th(n,γ) surrogate measurement and can be seen in fig. 9, but affects only the lowest data point, which is now 50% lower.

Fig. 10 shows the surrogate reaction measurements for ^{230}Th(n,γ) cross section. Since the total cross section is unknown we could not extract the TALYS input parameters that reproduce it. Instead we used the same input parameters as for the ^{232}Th(n,γ) to obtain the compound nucleus formation cross section for ^{230}Th. No direct measurements have been performed and this is reflected in the various evaluated databases, which differ by an order of magnitude. It should be stressed that the (^{3}He,^{4}He) surrogate reaction uses a heavier projectile and has not been validated thus the extracted cross section could be an overestimate.

The results for the ^{231}Pa(n,γ) surrogate cross section can be seen in fig. 11. A similar procedure to the ^{230}Th nucleus was used to calculate the compound nuclear formation cross section using TALYS pure OMP calculations. Data points higher than 600 keV are not presented since the presence of the a low fission threshold at ~600 keV will lead to an overestimate of the cross section due to the weighting of fission gamma rays that we are unable to correct for. At lower energies (< 400 keV), the surrogate method may be unreliable as we have seen in the case of ^{232}Th(n,γ). The two data points nearest 500 keV may therefore be the most reliable values. Since the evaluated databases disagree by an order of magnitude this measurement ought to help to heavily constrain theory even in such a narrow energy range. Again it should be noted that the (^{3}He,t) surrogate reaction has not yet been validated, so the extracted cross section could be an overestimate.

VI. CONCLUSIONS

Measurements of decay probabilities using the weighting function technique have been carried out in the actinide region for fertile final nuclei produced in the following reactions: ^{232}Th(d,p)^{233}Th, ^{232}Th(^{3}He,t)^{232}Pa and ^{232}Th(^{3}He,α)^{231}Th. These measurements have been combined with optical model calculations of compound nucleus formation cross sections to extract the neutron induced capture cross sections for ^{232}Th, ^{231}Pa and ^{230}Th via the surrogate method. Since the direct (n,γ) cross section for ^{232}Th is well known, a comparison of the indirect and direct measurements reveals a good agreement (< 15% difference) above 500 keV and below the onset of significant competition from fission (< 1 MeV). However, below 500 keV there is a discrepancy which increases towards lower energies and can be as high as 400%. This discrepancy probably occurs for two reasons: Firstly, the mismatch in spin distributions between the indirect and direct reactions leading to an overestimation of the cross section because decay of higher final nuclear *l*-waves favor decay by gamma emission. Secondly, the finite resolution of silicon detectors smoothes out the step function at the neutron binding energy that we are attempting to measure and thus the measured decay probabilities are the most incorrect in this region where the decay probability is varying extremely rapidly.

The question then arises as to why our surrogate ^{232}Th(n,γ) cross section data show good agreement with the direct measurements in the 500 keV-1 MeV range, when other (n,γ) surrogate measurements (e.g. Scielzo et al.[10]) do not. This may be due to the fact that level densities in the actinides are higher and thus decay probabilities are not as sensitive to differences in entry spin distributions as in the lanthanides. Furthermore, extracting decay probabilities by weighting the statistical gamma-rays could potentially be a more accurate technique than using high-resolution gamma spectroscopy of low-lying states to detect the residual nucleus because there is no bias placed on the spin(s) of the final states in the cascade. This could be especially important for actinide nuclei where the low-lying gamma transitions are often strongly internally converted and cannot be easily detected.

The surrogate technique has the potential to make reasonably accurate extraction of (n,γ) cross section information in a certain energy range. However, it must be used with caution. At lower energies (< 500 keV), it may not be appropriate to use the technique, and in actinide nuclei the gamma contribution from fission events should be subtracted at energies above the fission threshold, ideally with the aid of high-efficiency fission fragment detectors in the experimental set-up. Furthermore, the higher the mass of the projectile, the greater the maximum angular momentum brought into the final system and the greater the likelihood of an overestimation of (n,γ) cross sections due to spin distribution mismatch effects. For this reason (d,p) and (p,d) reactions look to be the best candidates for surrogate experiments. If rare actinide nuclei could be produced in inverse kinematics using the next generation of radioactive beam facilities such as FRIB (Facility for Rare Isotope Beams), Spiral2 (Système de Production d'Ions Radioactifs en Ligne), etc. then the surrogate technique could be used to make a whole range of measurements which remain difficult at the present time.

ACKNOWMEDGMENTS

We would like to thank the staff at the Oslo Cyclotron Laboratory for providing the stable and high-quality deuterium and ^{3}He beams during the experiment and the Lawrence Livermore National Laboratory for providing the ^{232}Th target.

This work was supported by the CNRS energy program PACEN (GEDEPEON), the Norwegian Research Council, and the US department of Energy under contract number DE-AC52-07NA27344.

BIBLIOGRAPHY

[1] J. Cramer and H. Britt, Nucl. Sci. Eng. **41** 177 (1970).
[2] M. Petit *et al.*, Nucl. Phys. **A735** 345 (2004).
[3] B.L. Goldblum, *et al,* Phys. Rev. C **80,** 044610 (2009).
[4] G. Kessedjian, B. Jurado, *et al.,* Physics Letters B 692 297 (2010).
[5] S. Boyer *et al.*, Nuc. Phys. **A775** 175 (2006).
[6] J.M. Allmond *et al.*, Phys. Rev C **79**, 054610 (2009).
[7] C. Plettner *et al*., Phys. Rev. C **71** 051602(R) (2005).
[8] B.F. Lyles *et al.*, Phys. Rev. C **76** 014606 (2007).
[9] J. Escher, F.S. Dietrich *et al.,* Phys. Rev. C **74** 054601 (2006).
[10] R. Hatarik *et al.,* Phys. Rev.C **81** 011602 (2010).
[11] N.D. Scielzo *et al.,* Phys. Rev. C **81** 034608 (2010).
[12] Till von Egidy and Dorel Bucurescu, Phys. Rev. C **72** 044311 (2005).
[13] M. Guttormsen, A. Bürger, T.E. Hansen and N. Lietaer. Nucl. Instrum. Meth. Phys. Res. **A648** 168 (2011).
[14] J.N. Wilson *et al*., Nucl. Instrum. Meth. Phys. Res. **A511** 388 (2003).
[15] A. Borella et al., Nucl. Instr. Meth. A577 626 (2007).
[16] O. Häusser, M.A. Lone, T.K. Alexander, S.A. Kushneriuk, and J. Gascon, Nucl. Instrum. Meth. Phys. Res. **A213** 301 (1983).
[17] A.J. Koning and J.P. Delaroche, Nucl. Phys. **A713** 231 (2003).
[18] G. Aerts, *et. al*, Phys. Rev. C **73** 054610 (2006).
[19] A. Borella et al., Nucl. Sci. Eng. 152 1 (2006).
[20] I. Sirakov et al., An. Nucl. Energy 35 1223 (2008).

FIGURE CAPTIONS

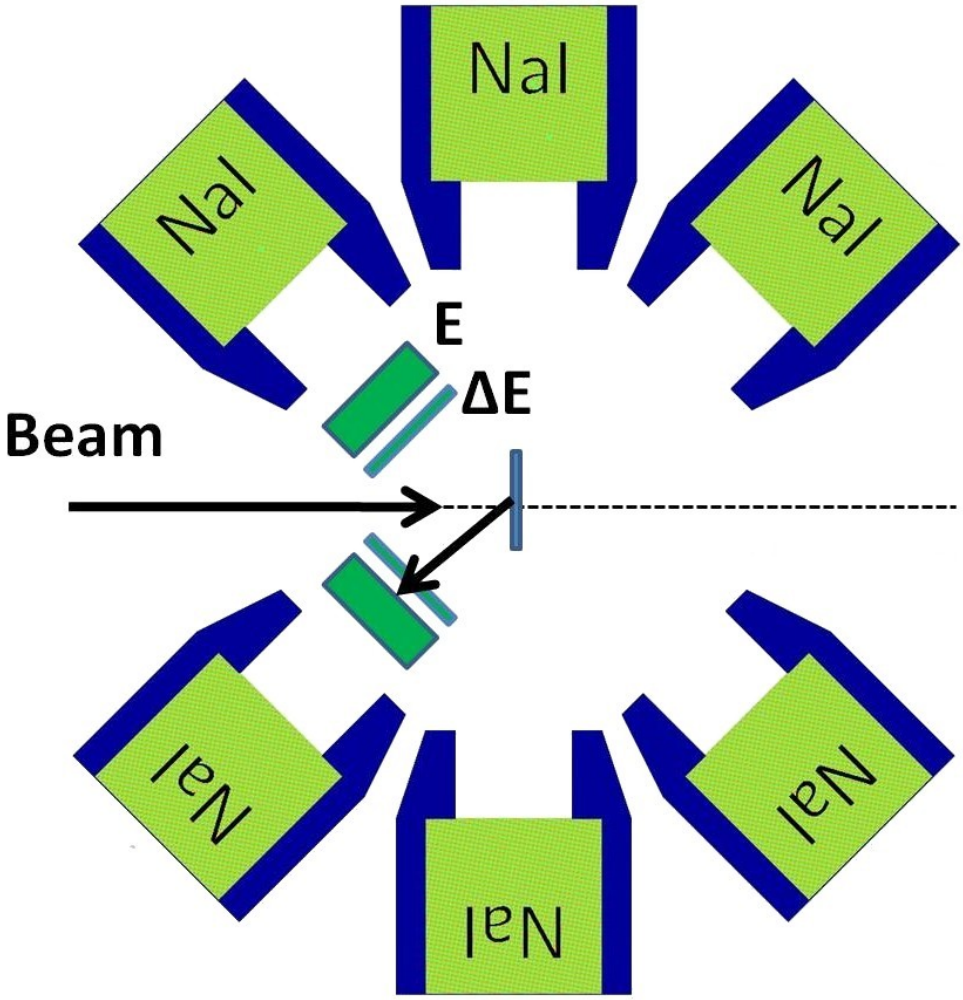

Fig. 1. (Color online) Schematic diagram of the experimental apparatus. The target was situated at the centre of the Cactus gamma detector array and the silicon ring for charged particle detection was placed at backward angles with respect to the beam at a distance of 5cm between the target and the front face of the Delta E detectors. The aluminum foil to protect the silicon detectors from Delta electrons is not shown.

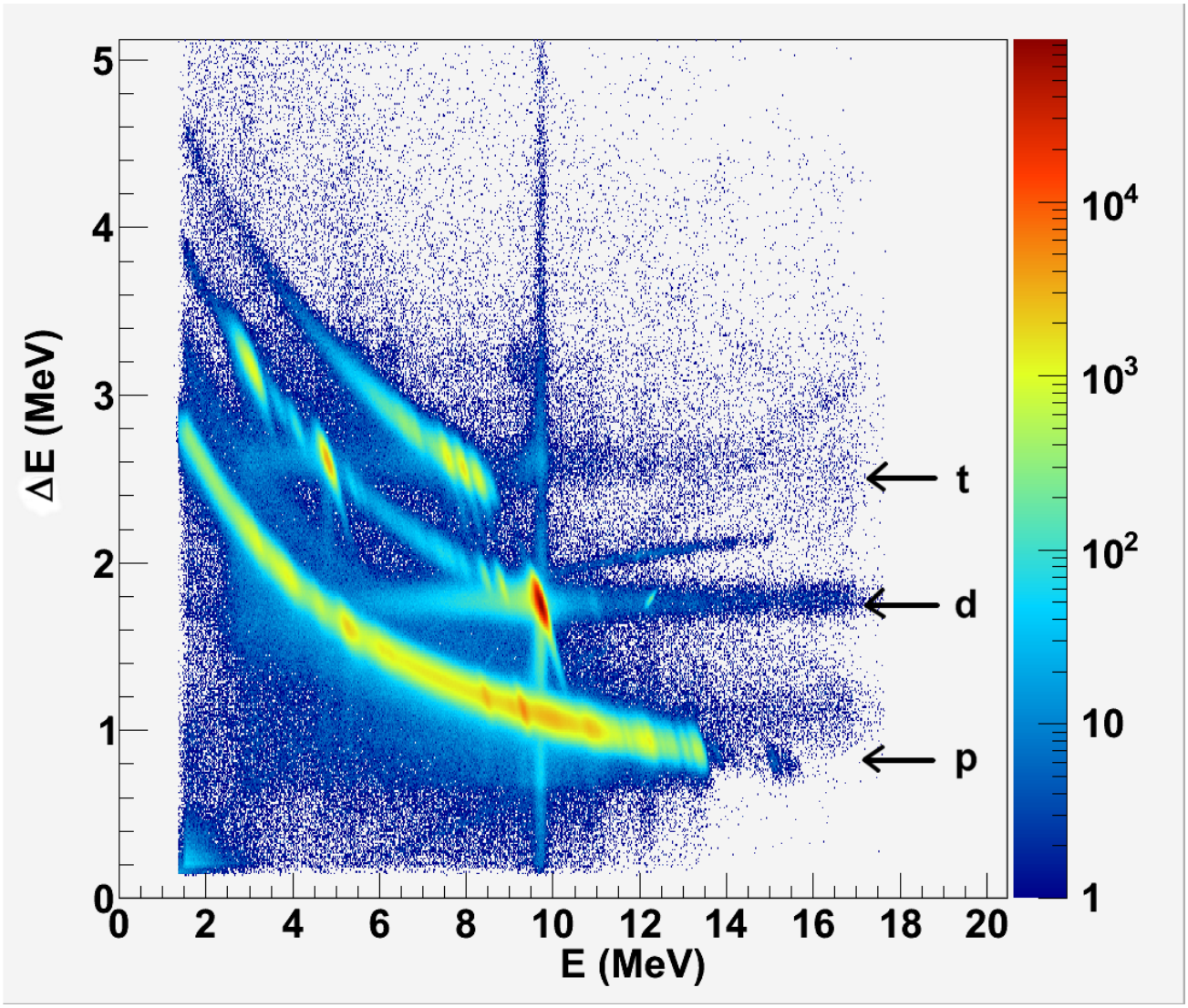

Fig. 2 (Color online) Energy deposited in the E vs DE detectors at 124 degrees in the Silicon ring for ^{232}Th(d,x) ejectiles, where E is the residual energy detected in the E detectors. Protons, deuterons and tritons (p,d and t) can be separated cleanly.

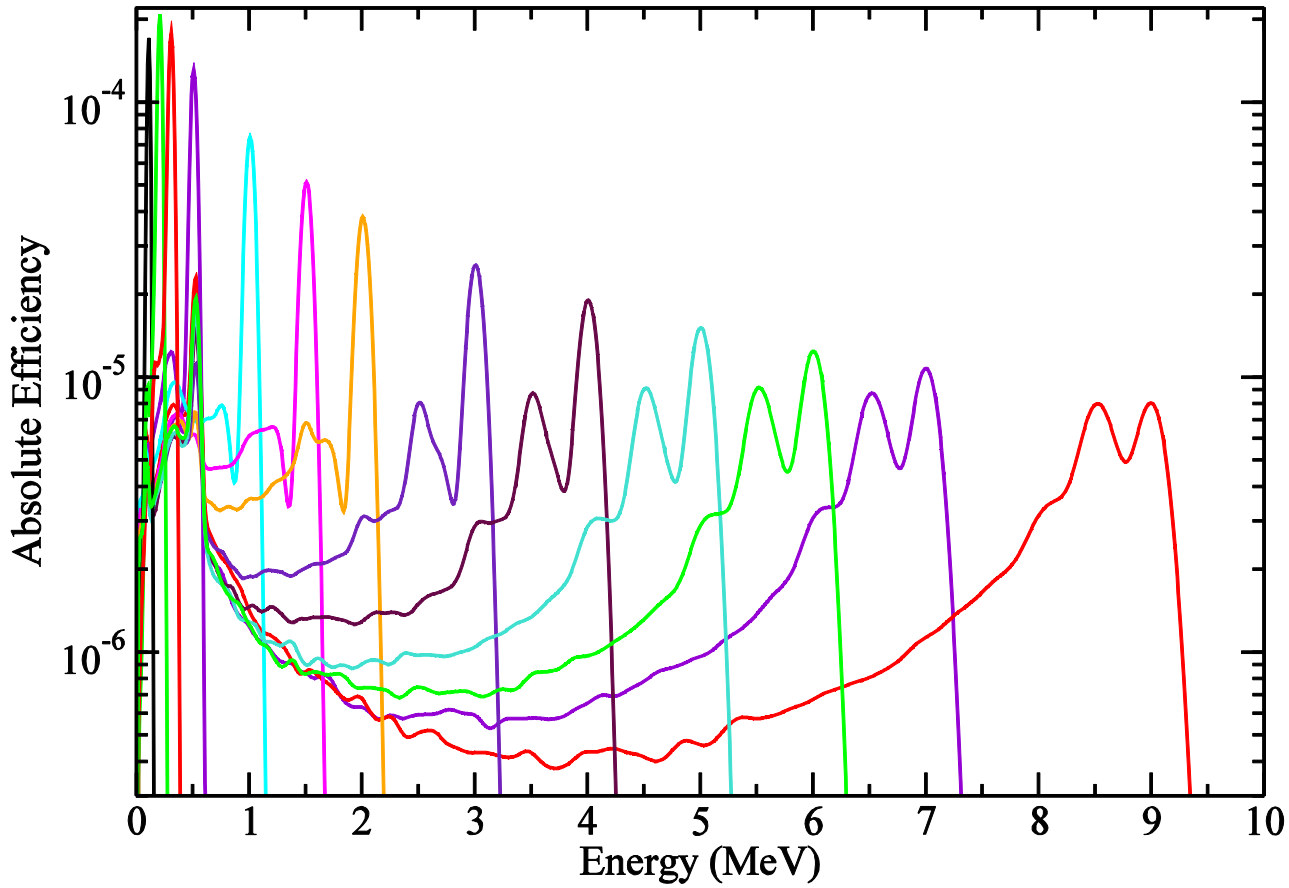

Fig. 3. (Color online) MCNP5 simulations of the response of the Cactus detector array to gamma rays with energies between 100 keV and 9 MeV. The detector resolution broadening function was taken from a fit to measured width data from photo-peaks of energies up to 3.8 MeV.

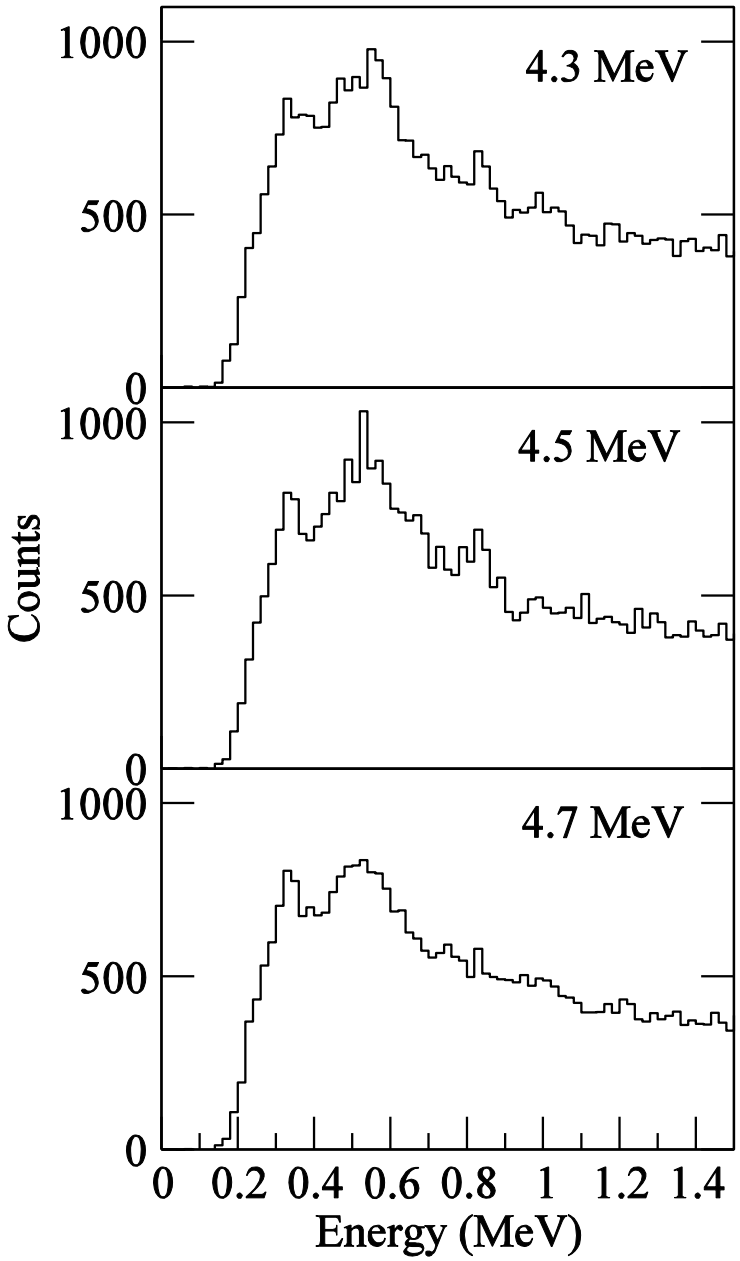

Fig. 4. The low energy (< 1.5 MeV) part of the observed gamma spectra detected in coincidence with ^{233}Th final nuclei of excitation energies of 4.3, 4.5 and 4.7 MeV, below the neutron binding energy at S_n=4.786 MeV. The excitation energy bins are 70 keV wide.

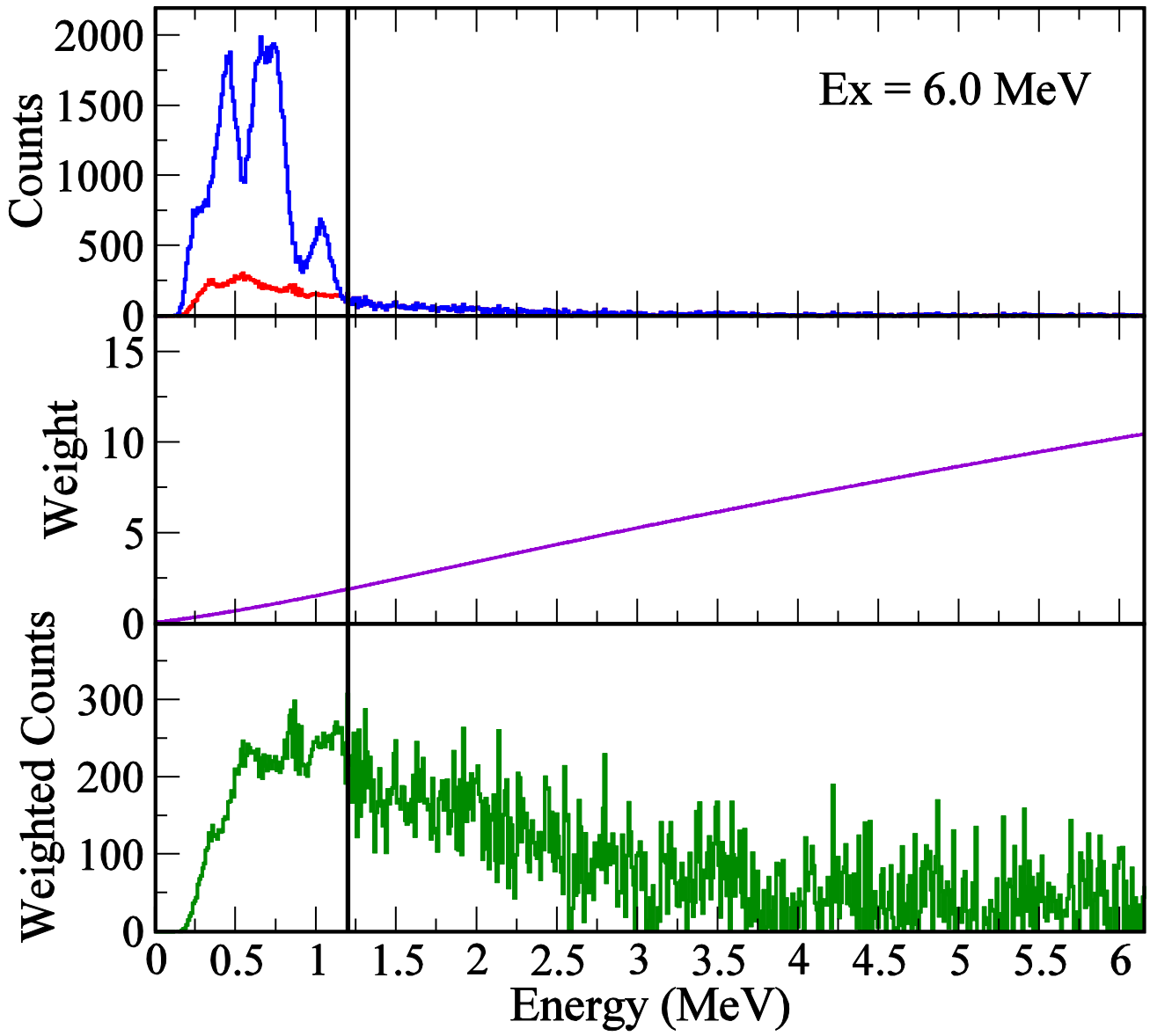

Fig. 5. (Color online) The extrapolation technique proposed to correct for the equivalent of (n,n') events. The "worst" case at E_x= 6.0 MeV is shown, where the threshold (solid black line) must be placed at (6.0-4.786 = 1.21 MeV) to eliminate gamma rays from these events from the weighting. The gamma spectrum is extrapolated below this threshold from knowledge of the spectral shape, which is not assumed to change with E_x. The top panel shows the observed gamma spectrum (blue histogram), with extrapolation below threshold (red histogram). The middle panel shows the weighting function calculated for E_x= 6.0 MeV and the bottom panel shows the weighted composite spectrum from which the decay probability at this energy is obtained.

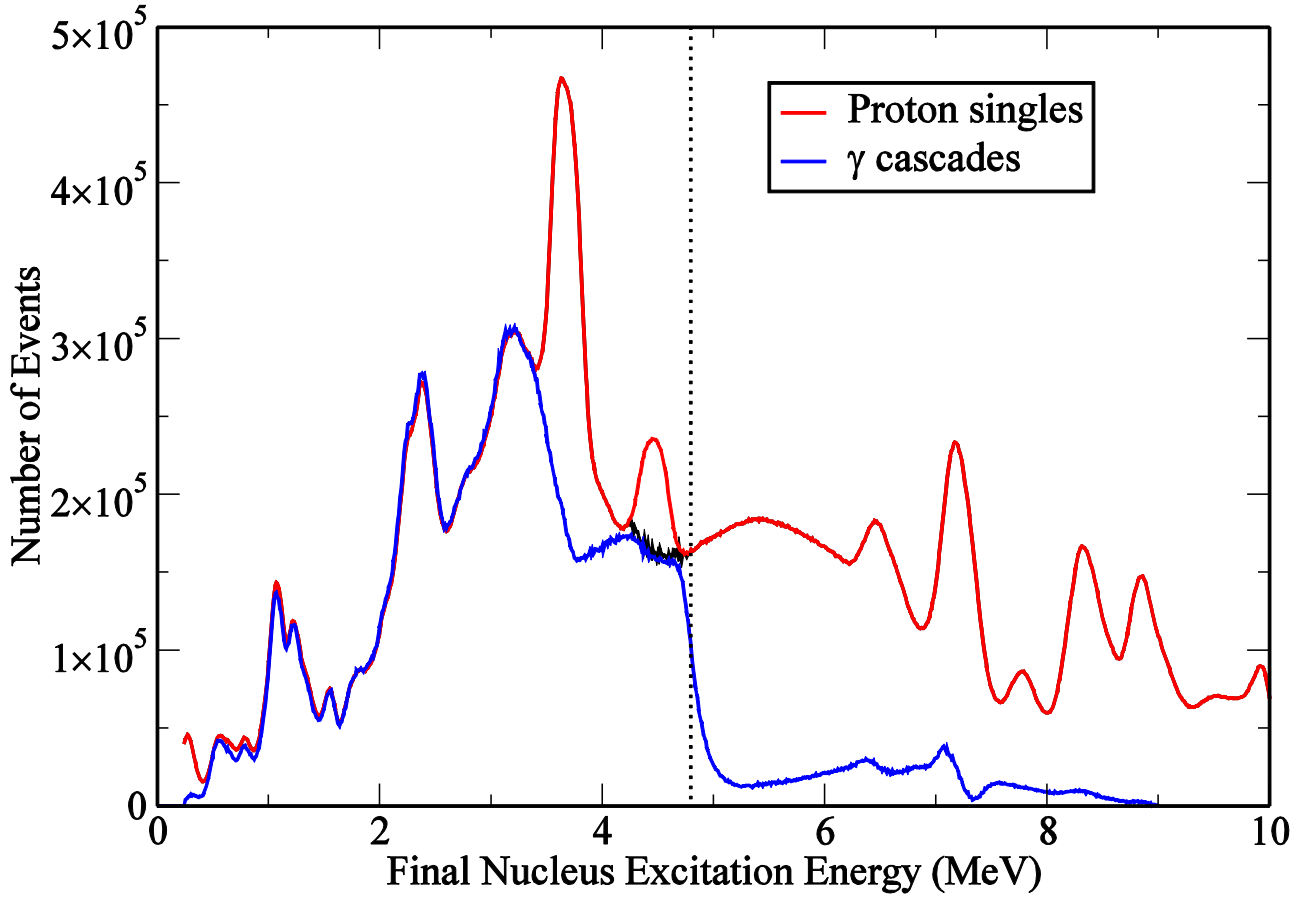

Fig. 6. (Color online) The number of protons from the ^{232}Th(d,p) reaction detected in the Silicon Ring (red curve) compared to the number of cascades decaying to the ^{233}Th ground state, counted using the weighting function technique (blue curve). The neutron separation energy S_n=4.876 MeV is shown with the dotted line. The proton "singles" peaks at 3.8 MeV and 4.5 MeV correspond to contamination from (d,p) reactions on ^{16}O in the target. The contribution from the first excited state can be subtracted from fits to the associated gamma spectra (black line).

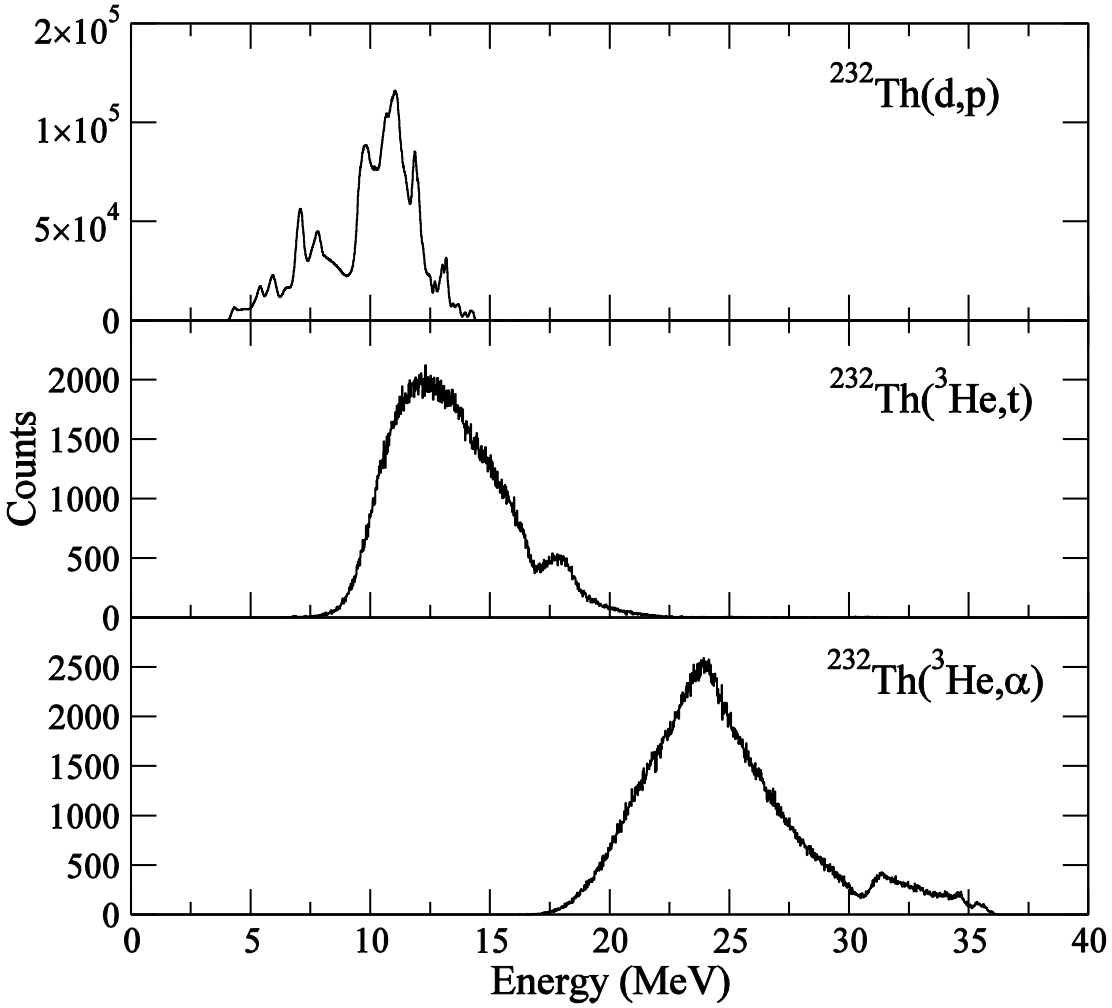

Fig. 7. Total detected energy in the lab frame of the ejectiles in the Silicon Ring for the three reactions studied in this work. A coincidence of at least one gamma ray in the Cactus spectrometer with each particle was required. The particle energy corresponding to the neutron binding energy in the residual nucleus can be seen in each spectrum at approximately 9.5, 17.5 an d 32.5 MeV for p, t and α respectively.

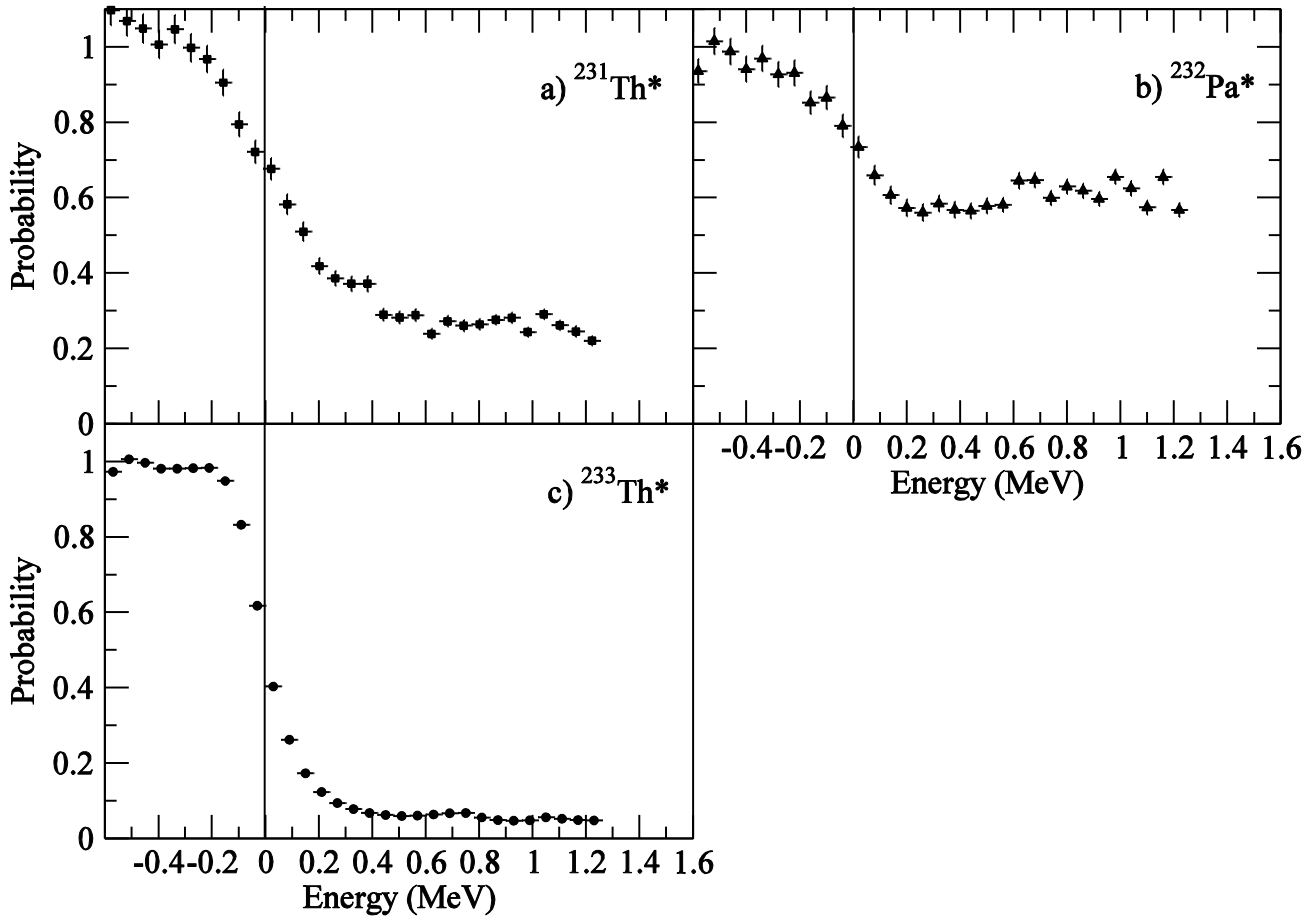

Fig. 8. The measured gamma decay probabilities for a) ^{231}Th, b) ^{232}Pa, and c) ^{233}Th for equivalent neutron energies, E_n, between 0 – 1 MeV. The corresponding neutron separation energies at equivalent E_n=0 are 5.118 MeV, 5.549 MeV and 4.786 MeV respectively. The error bars are statistical errors only. Relative systematic uncertainties introduced from imperfect weighting could be as large as 2% and absolute systematic uncertainties are estimated as 5%.

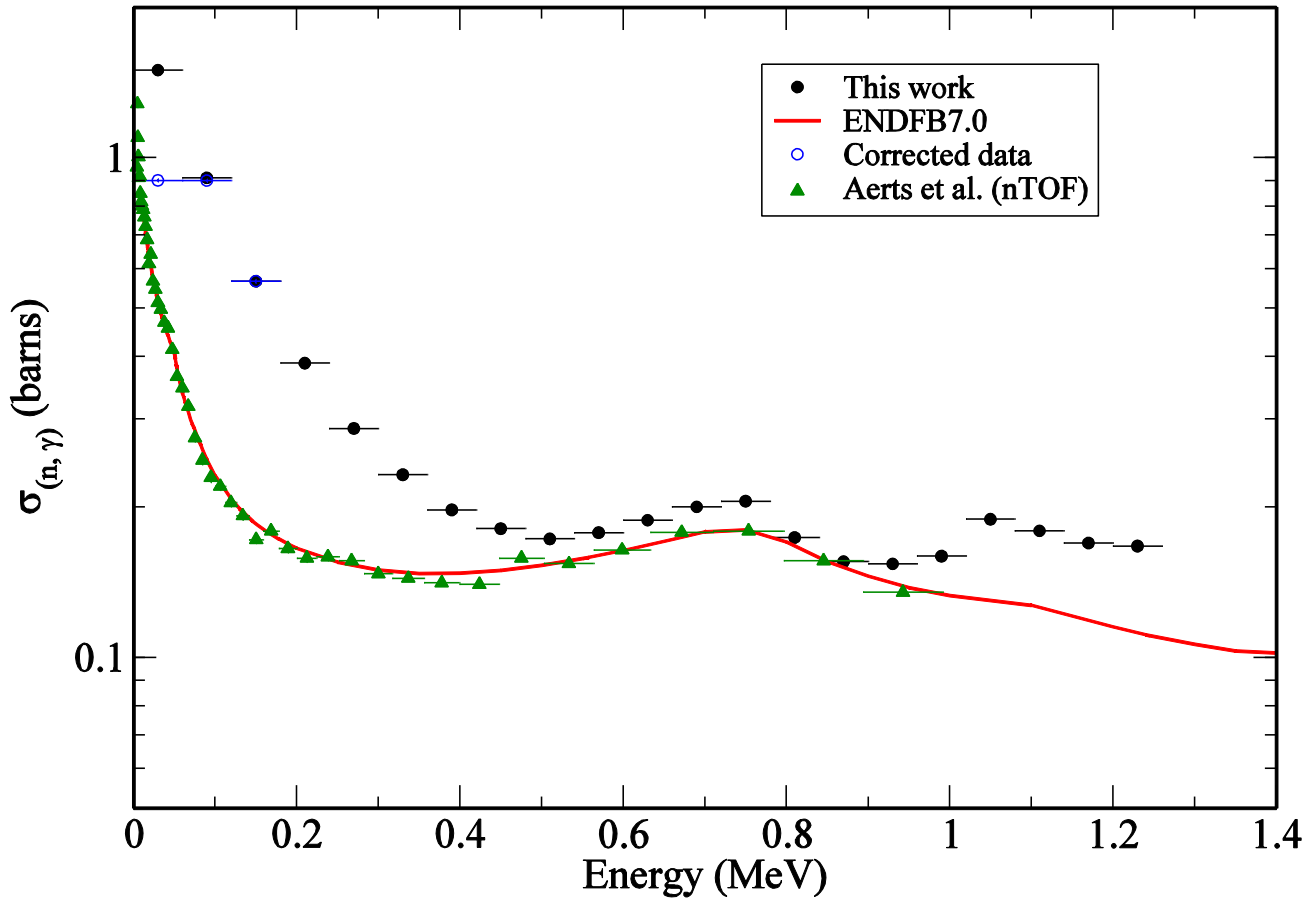

Fig. 9. (Color online) The indirect ^{232}Th(n,γ) cross section measured with the surrogate method using the ^{233}Th(d,p) reaction. The compound nucleus formation cross section was obtained from TALYS optical model calculations with input parameters adjusted to accurately reproduce the experimental total cross sections. The results are compared to the ENDFB7 database and the direct neutron-induced data by Aerts. *et al.* measured at the nTOF facility.

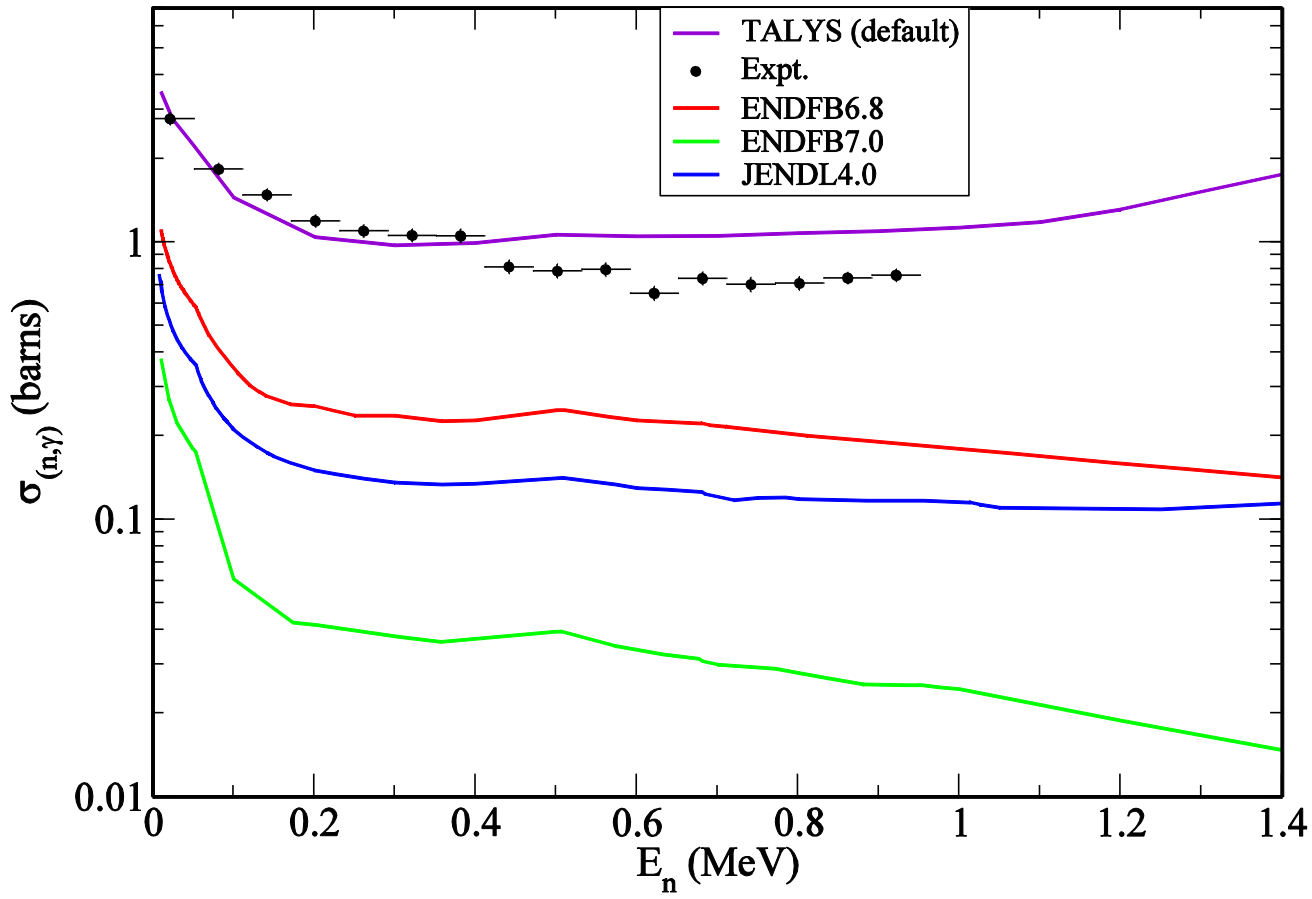

Fig. 10. (Color online) The indirect ^{230}Th(n,γ) cross section obtained with the surrogate method using the ^{232}Th(^{3}He,^{4}He) reaction. The compound nucleus formation cross section was obtained from TALYS optical model calculations with input parameters identical to those for the ^{232}Th(n,γ) measurement. The error bars are statistical errors only. The systematic errors (~20%) due to introduction of the model-dependent compound nucleus formation cross section are not included.

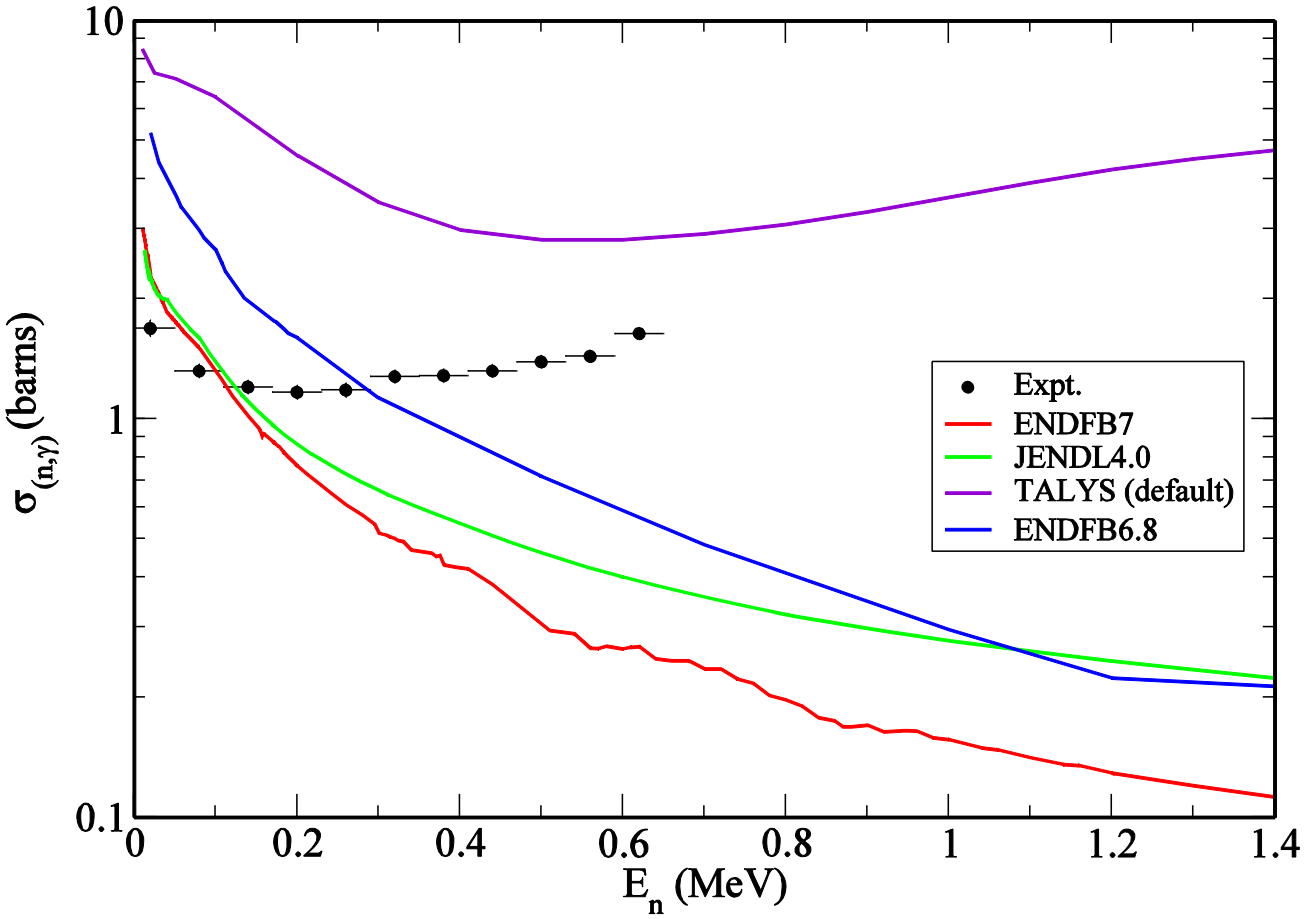

Fig. 11. (Color online) The indirect ^{231}Pa(n,γ) cross section obtained with the surrogate method using the ^{232}Th(^{3}He,t) reaction. The compound nucleus formation cross section was obtained from TALYS optical model calculations with input parameters identical to those for the ^{232}Th(n,γ) measurement. The error bars are statistical errors only. The systematic errors (~20%) due to introduction of the model-dependent compound nucleus formation cross section are not included.